*Romanian Reports in Physics, Vol. 67, No. 3, P. 890–914, 2015*

**CONDENSED MATTER**

# APPLICATION OF THE TIME-TEMPERATURE SUPERPOSITION PRINCIPLE TO CONCENTRATED MAGNETIC NANOFLUIDS

DANIELA SUSAN-RESIGA[1, 2]

[1]West University of Timisoara, Faculty of Physics, Timisoara, Romania
[2] Romanian Academy – Timisoara, Laboratory of Magnetic Fluids, Center for Fundamental and Advanced Technical Research, Timisoara

*Received July 23, 2014*

*Abstract.* The time-temperature superposition principle (TTSP), usually applied in case of viscous-elastic linear polymers, was extended to concentrated magnetic fluids taking into account also the influence of an applied magnetic field. There were investigated two samples of magnetic nanofluid based on transformer oil, with magnetite nanoparticles, having the saturation magnetizations $M_s$ = 600 G and respectively $M_s$ = 1100 G. Using the data measured for the loss modulus in the Frequency Sweep dynamic test at temperatures between 20°C and 70°C, a master curve of the loss modulus *vs.* frequency was obtained, which shows the simple thermo-rheological character of these magnetic nanofluids.

*Key words*: magnetic fluid, superposition principle, rheology, magnetorheology.

## 1. INTRODUCTION

Magnetically controllable fluids-ferrofluids and magnetorheological fluids-manifest simultaneously fluid and magnetic properties [1, 2]. Both the magnetic and flow properties are strongly related to the composition of the fluids, in particular to the size range and volume fraction of magnetic particles [3]. Recent progress in the field reveals how the composition of magnetizable fluids is designed to fulfill the requirements of the envisaged application [4], such as high saturation magnetization for rotating MF seals [5] or magnetic field controlled effective viscosity [6, 7] for magnetorheological (MR) devices. High magnetization magnetic nanofluids and nano-micro composite fluids for rotating seal applications [8] have to withstand long-term (several years) action of intense and strongly non-uniform magnetic fields, while keeping adequate flow properties.

Investigating the rheological behavior of magnetic fluids is important in establishing strategies for their exploitation. For complex viscoelastic materials, by

measuring data at a few temperatures, TTSP can be applied to generate a master curve that can predict the behavior at a reference temperature covering many time or frequency decades. Materials for which this technique is applicable are called thermo-rheologically simple ones [9].

A master curve of a dynamic viscoelastic property, for example the loss modulus $G''$ as a function of angular frequency $\omega$ based on data obtained at different temperatures $T$ is obtained by representing:

$$b_T \; G''(T) \; versus \; \omega a_T,$$

using a logarithmic scale for both axes. Here $G_r'' = b_T G''(T)$ is called reduced loss modulus and $\omega_r = \omega a_T$ is the reduced frequency.

The TTSP concept can be expressed as an equation that relates the property measured at a reference temperature $T_0$ to the one measured at a temperature $T$ and then shifted to $T_0$, so for the loss modulus $G''$:

$$b_T G''(T, \omega, a_T) = G''(T_0, \omega) \quad \text{or} \quad G_r''(T, \omega_r) = G''(T_0, \omega). \tag{1}$$

where $a_T, b_T$ are the horizontal and vertical shift factors. Their temperature dependence can be expressed as:

– the Arrhenius model:

$$a_T = \exp\left[\frac{E_a}{R}\left(\frac{1}{T} - \frac{1}{T_0}\right)\right] \quad [9–11], \tag{2}$$

$$b_T = \frac{1}{\exp\left[\frac{E_b}{R}\left(\frac{1}{T} - \frac{1}{T_0}\right)\right]} \quad [10–12], \tag{3}$$

where $E_a$ = retardation activation energy, $E_b$ = relaxation activation energy and $T_0$ = reference temperature;

– the Williams-Landel-Ferry (WLF) model, valid in the ($T_g$, $T_g$ + 100 K) temperature domain, where $T_g$ = the glass transition temperature:

$$a_T = 10^{\frac{-c_1 (T - T_0)}{c_2 + (T - T_0)}} \quad [9–14], \tag{4}$$

and taking into account the relationship between the two coefficients resulting from (2) and (3) we get:

$$b_T = 10^{\frac{+c_3 (T - T_0)}{c_4 + (T - T_0)}} \quad [12], \tag{5}$$

with $c_1$, $c_2$, $c_3$, $c_4$ as empirical constants. Also, according to the Bueche-Rouse [15, 16] theory of linear viscoelasticity for unentangled polymer solutions and melts, $b_T$ depends on the density of the sample, not only on temperature:

$$b_T = \frac{\rho_0 T_0}{\rho T}, \tag{6}$$

where $\rho_0$ is the density at the reference temperature $T_0$, and $\rho$ is the density at temperature T.

The temperature dependence of the vertical shift factor $b_T$ was reported in literature as being generally weaker than that of the horizontal shift factor $a_T$, and sometimes $b_T = 1$, independent of temperature [9, 11, 14].

Sometimes these factors are determined analytically by fitting the entire set of data obtained, the data being shifted both vertically and horizontally, and thus masking, by averaging over the entire domain of frequencies, the discrepancies that happen when applying TTSP. If both factors are obtained in this manner, none of them has any physical meaning [9]. TTSP has been validated not only on polymers [9, 10, 11, 14, 17], but also on honey [12].

By applying TTSP for the rheological properties of a certain fluid (with thermo-rheological simple character), the resulting advantages are the following:

- The values for certain rheological properties (loss modulus *G''* or storage modulus *G'*, loss compliance *J''* or storage compliance *J'*, absolute value of complex modulus $|G^*|$, of loss tangent $\tan\delta$ etc.) are determined at low angular frequencies, where it is difficult to do measurements and take long periods of time.
- These values may be determined for any temperature within the investigated domain.

In this paper, using a Physica MCR-300 rheometer, we report on the rheological behavior of two concentrated magnetic nanofluid samples based on transformer oil with magnetite nanoparticles, having saturation magnetizations $M_s$ = 600 G and respectively $M_s$ = 1100 G, as a function of various parameters (shear rate, temperature, time, angular frequency, induction of the applied magnetic field), establishing the thermo-rheological character of the samples both in the absence and in the presence of an external magnetic field.

The magnetic fluids with high saturation magnetization ($M_s$ > 500 G) and relatively low viscosity are required in many applications, especially MF rotating seals. The preparation procedure of MFs with high concentrations of magnetic nanoparticles has to solve the increasing difficulties in securing their stability, even in the absence of an external magnetic field [18, 19]. To ensure the long-term

stability of a magnetic fluid, the energy of thermal motion in the fluid must exceed that of the attractive forces between particles even at close packing [20, 21, 5]. The composition of MFs and their structure at nanoscale, such as volume fraction of magnetic nanoparticles, particle size and shape, particle size distribution, interactions between particles and agglomerate formation influence the flow behavior of MF up to highest values of hydrodynamic volume fraction [1, 20]. For concentrated MFs the dependency of dynamic viscosity on the particle volume fraction and on temperature in the absence of an external magnetic field was analyzed in [5]. By correlating these data with those obtained from TEM, DLS and magnetogranulometry, it was evidenced the agglomeration of particles in clusters of ~1.3 particles per cluster, due to van der Waals interactions.

In the present work both rotational and oscillatory tests were performed, followed by the application of the TTSP principle, thus verifying the thermorheologically simple character of these samples. At least one of the shift factors was determined, namely the horizontal shift factor $a_T$ (using formula (2)), by investigating the temperature dependence of the dynamic viscosity. For the more diluted sample it was possible to determine experimentally the vertical shift factor $b_T$ (using formula (6)), by measuring the density's dependency on temperature in the investigated domain. The reference temperature chosen was $T_o$ = (20 + 273.15) K.

The preservation of the flow behavior of magnetic fluids when the temperature or the induction of the applied magnetic field changes it is important for most of engineering applications like magnetic fluid rotating seals.

## 2. EXPERIMENTAL

### 2.1. SAMPLES

The rheological study was done on two samples of magnetic nanofluids based on transformer oil: MF/UTR-30, with saturation magnetization $M_s$ = 600 G, and MF/UTR-30, with $M_s$ = 1100 G. The MF/UTR samples were obtained using the chemical coprecipitation synthesis procedure of magnetite nanoparticles, followed by sterical stabilization with oleic acid (product 100471 Merck). The stabilized particles were then dispersed in UTR (MOL TO 40A) without any surfactant excess, following the procedure developed by Doina Bica [22, 18, 19] and briefly described also in [5].

The saturation magnetizations were determined at room temperature using a vibrating sample magnetometer (VSM 880, ADE Technologies, USA) in the 0–800 kA/m domain of magnetic field intensities.

### 2.2. EXPERIMENTAL SETUP

For the rheological and magneto-rheological investigations a Physica MCR-300 Anton Paar rheometer was used. For the MF/UTR-30, $M_s$ = 600 G sample (less concentrated) we used the double gap cylinder rheological cell, and the measurements were done only in the absence of a magnetic field. However, for the MF/UTR-30, $M_s$ = 1100 G, the more concentrated and more viscous sample, we could perform measurements in the presence of an external magnetic field, using the parallel plate magnetorheological cell with a diameter of 20 mm. For each measurement a new quantity of sample was inserted, ensuring the time laps to reach the required temperature for investigation. Density measurements were done using a digital instrument.

## 3. RESULTS AND DISCUSSION

For both samples three types of rheological tests were performed, at temperatures $t$ = 20, 30, 40, 50, 60, 70°C:

- Flow / viscosity curves in the $\dot{\gamma} = (1-1000)\ \mathrm{s}^{-1}$ domain for shear rate;
- Amplitude sweep test with fixed angular frequency $\omega = 1\ \mathrm{s}^{-1}$;
- Frequency sweep test with fixed strain amplitude $\gamma_A = 1$.

Sample: MF / UTR-30, 4T; $M_s$ = 600 G;
Code: 100108-101 from 20.02.2008.

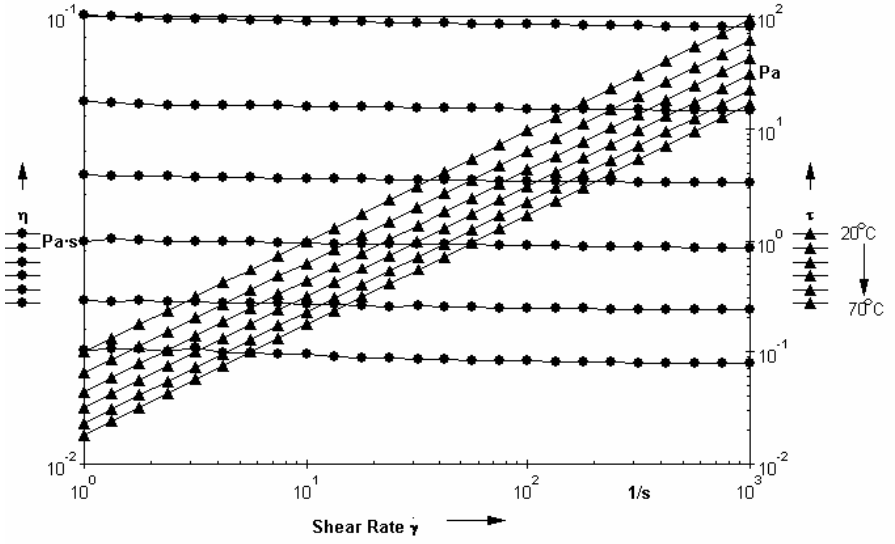


Fig. 1 – Flow / viscosity curves at $t$ = 20, 30, 40, 50, 60, 70°C, in shear rates range $\dot{\gamma} = (1-1000)\ \mathrm{s}^{-1}$ – sample MF / UTR-30, $M_s$ = 600 G.

Flow / viscosity curves at temperatures $t$ = 20, 30, 40, 50, 60, 70 °C, in the $\dot{\gamma} = (1 - 1000)$ s$^{-1}$ domain for shear rate are presented in Fig. 1.

From Fig. 1 one can see that sample MF/UTR-30, $M_s$ = 600 G has a roughly Newtonian behavior, and the viscosity decreases with temperature.

Figure 2 shows the results of amplitude sweep tests at the same temperatures.

We can see from Fig. 2 that *G" > G'*, denoting the liquid behavior of this sample. The storage modulus *G'* has low values, close to the measurement limit of the rheometer. Complex viscosity $|\eta^*|$ is independent of strain $\gamma$, which confirms the Newtonian character of the rheological behaviour revealed by the rotational test (viscosity curves). There is no critical strain, G" being independent of strain. Therefore the next oscillating test, frequency sweep, can be performed at any fixed value for the strain amplitude. We chose $\gamma_A = 1$.

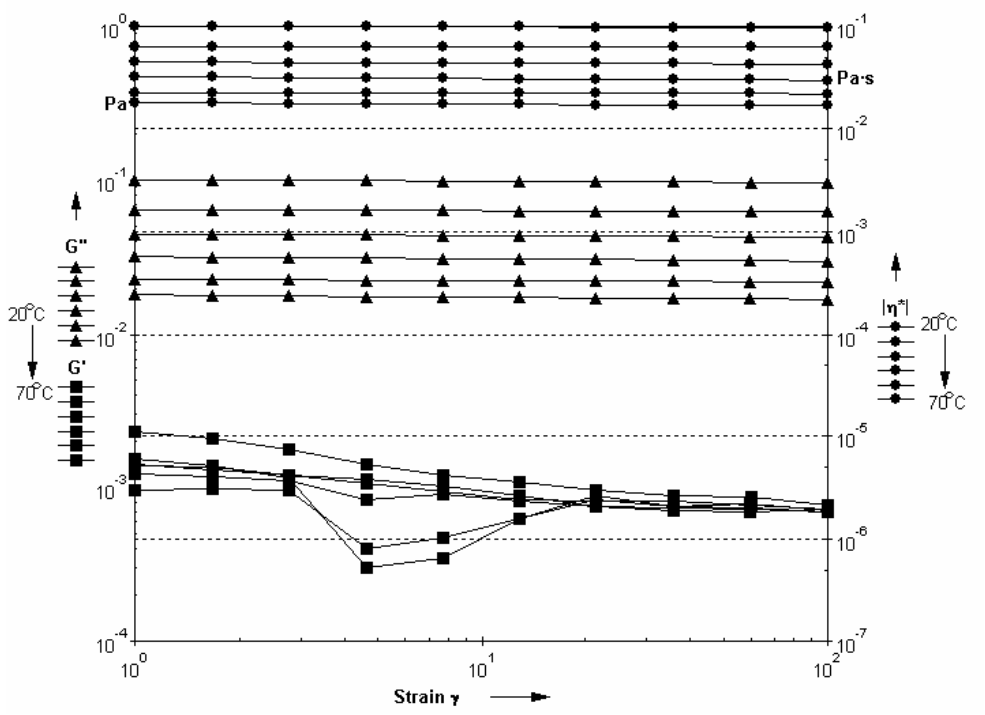


Fig. 2 – Amplitude sweep at the same temperatures – MF / UTR-30, $M_s$ = 600 G.

Frequency sweep at $\gamma_A = 1$, at the same temperatures for sample MF / UTR-30, $M_s$ = 600 G gives the *G" = G"*($\omega$) curves shown in Fig. 3.

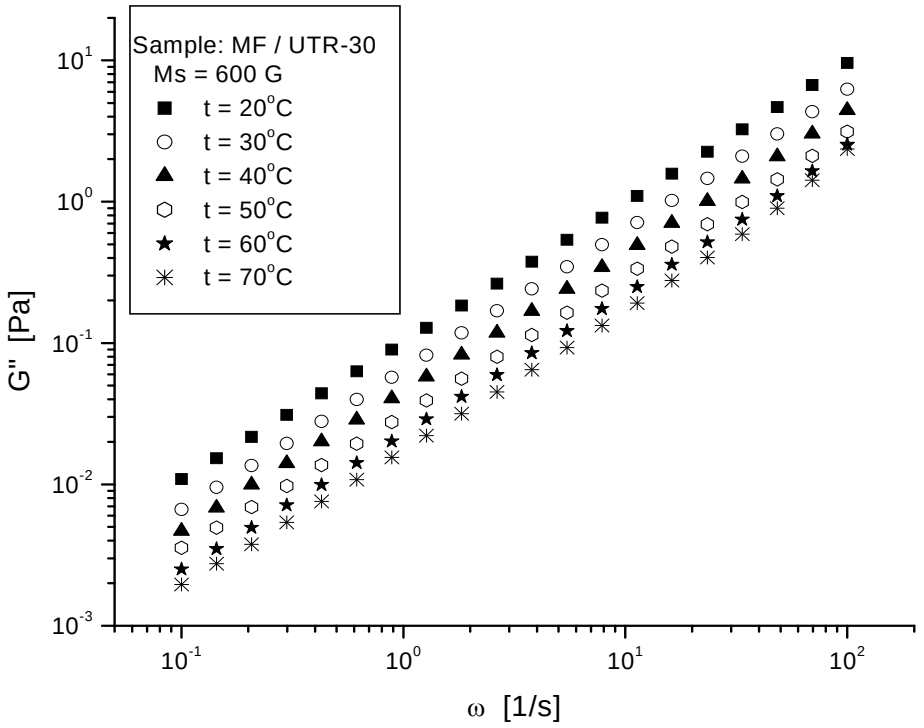


Fig. 3 – Results for frequency sweep tests at the same temperatures – sample MF/UTR-30, $M_s$ = 600 G.

For this sample, both shift factors (horizontal $a_T$, respectively vertical $b_T$) were determined experimentally. From fitting $\eta=\eta(t)$ data with Arrhenius type formula (2) it follows $a_T$ (Fig. 4):

$$a_T = \exp\left[\frac{E_a}{R}\left(\frac{1}{T}-\frac{1}{T_o}\right)\right],$$

where $E_a$ = activation energy of viscous flow, and $T_o$ = reference temperature. We chose $T_o$ = (20 + 273.15) K.

The values obtained for $a_T$ at the investigated temperatures decrease with temperature.

From density measurements (using a digital density meter) at various temperatures we determined the vertical shift factor $b_T$ (using formula (6)), which also decreases with temperature.

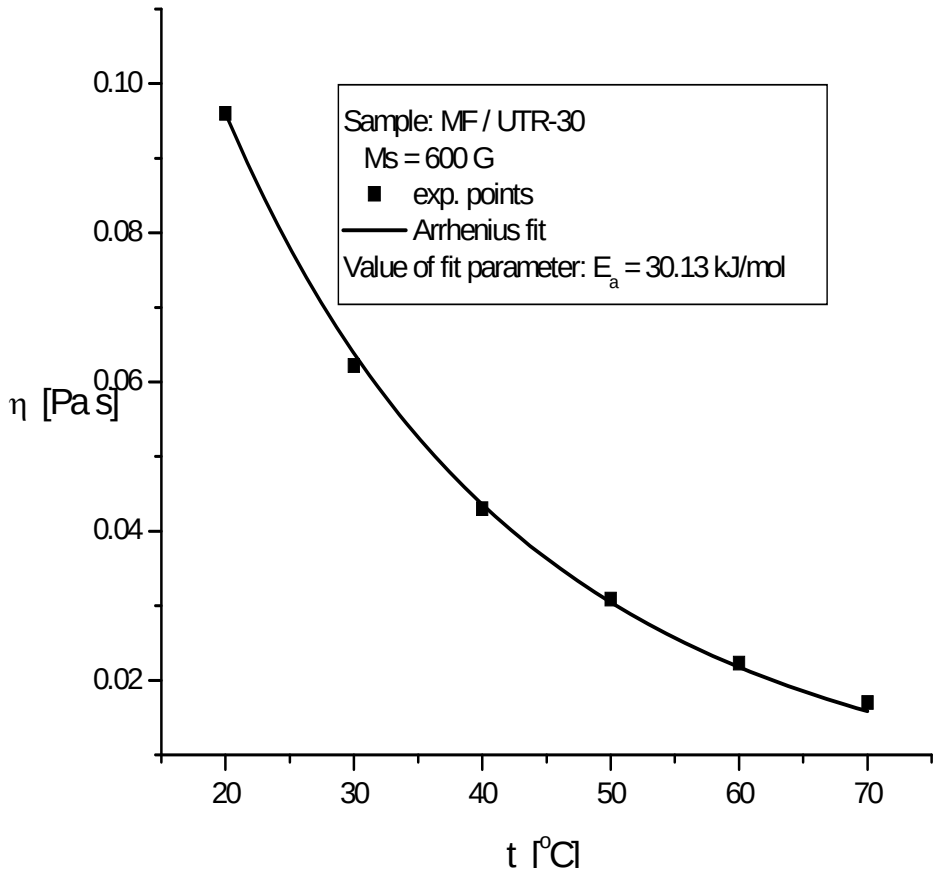


Fig. 4 – Fitting the temperature dependence of viscosity with an Arrhenius type formula – sample proba MF / UTR-30, $M_s$ = 600 G.

Performing the vertical and horizontal shifts, we get the master curve of Fig. 5.

Figure 6 illustrates the dependence of shift factors on temperature. Continuous and dashed lines represent fits with Arrhenius, respectively WLF models ($a_T$ was obtained by fitting data for viscosity-temperature with the Arrhenius type formula), values for the fitting parameters are shown in Table 1. Both models provide good correlations of the experimental data $a_T$, $b_T$ as a function of temperature. The dependence on temperature of $a_T$ is stronger than that of factor $b_T$, as it was specified in some recent works [9, 11, 14].

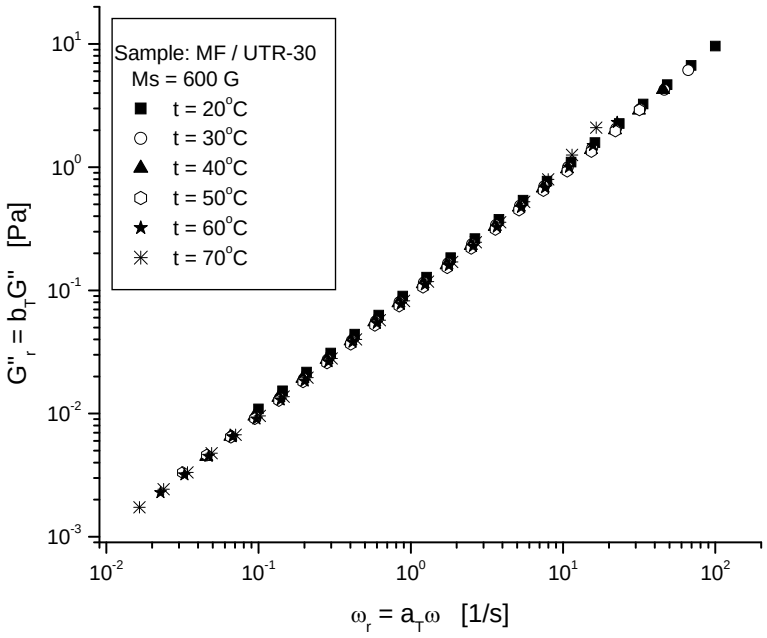


Fig. 5 – Master curve for sample MF / UTR-30, $M_s$ = 600 G.

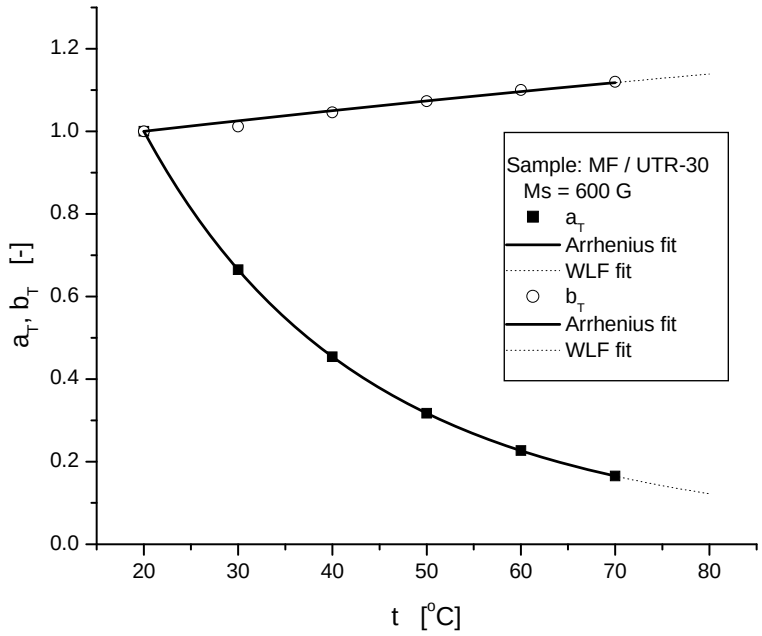


Fig. 6 – Temperature dependence of $a_T$, $b_T$ factors – sample MF / UTR-30, $M_s$ = 600 G.

*Tabel 1*

Fit equations (and coefficients regression) from Fig. 6

| MF / UTR-30, $M_s$ = 600 G | |
|---|---|
| Arrhenius model | WLF model |
| $\begin{cases} a_T = \exp\left[3624.05\left(\frac{1}{T}-\frac{1}{T_o}\right)\right], R^2 = 1 \\ b_T = \frac{1}{\exp\left[224.50\left(\frac{1}{T}-\frac{1}{T_o}\right)\right]}, R^2 = 0.981 \end{cases}$ | $\begin{cases} a_T = 10^{\frac{-5.37\ (T\ -\ T_o)}{293.15+\ (T\ -\ T_o)}},\ R^2 = 1 \\ b_T = 10^{\frac{+0.33\ (T\ -\ T_o)}{293.15+\ (T\ -\ T_o)}},\ R^2 = 0.981 \end{cases}$ |

Sample: MF / UTR-30, 4T; $M_s$ = 1100 G

Code: 100108-106 from 20.06.2008

For the concentrated sample MF / UTR-30, $M_s$ = 1100 G the same types of rheological tests were performed, at the same temperatures, both in the absence and presence of an applied magnetic field.

For this sample factor $a_T$ was determined in a similar fashion to the first sample's case, from correlating $\eta = \eta(t)$ data with the Arrhenius type formula, but $b_T$ was determined from a linear fit of log $G'' = f(\log\omega)$ data. Due to the sample being too viscous, we could not use a digital density meter to determine density at various temperatures.

In the case when both factors are determined from fitting data sets obtained from oscillation tests (*e.g.* $G'' = G''(\omega)$), then none of the factors has no physical meaning, and the results can mask any drift of the data from the master curve [9].

*Tests in the absence of a magnetic field*. From flow/viscosity curves of this sample for the same temperatures (Fig. 7), we can see that at $t$ = 20, 30, 40°C, the behavior is Newtonian only for small shear rates, after which it becomes shear thinning. This indicates the presence of particle agglomerates, evidenced also in [5], which are destroyed under intense shear. At temperatures larger than 40°C the behavior is Newtonian for the entire investigated shear rate domain, which shows that the particle agglomerates are also destroyed when the temperature increases.

From the results of the amplitude sweep test at the same temperatures and $B$ = 0 mT (Fig. 7), the behavior of an ideally viscous liquid is observed, the same as for the MF / UTR-30, $M_s$ = 600 G sample. Therefore we chose the same value $\gamma_A = 1$ for the frequency sweep test.

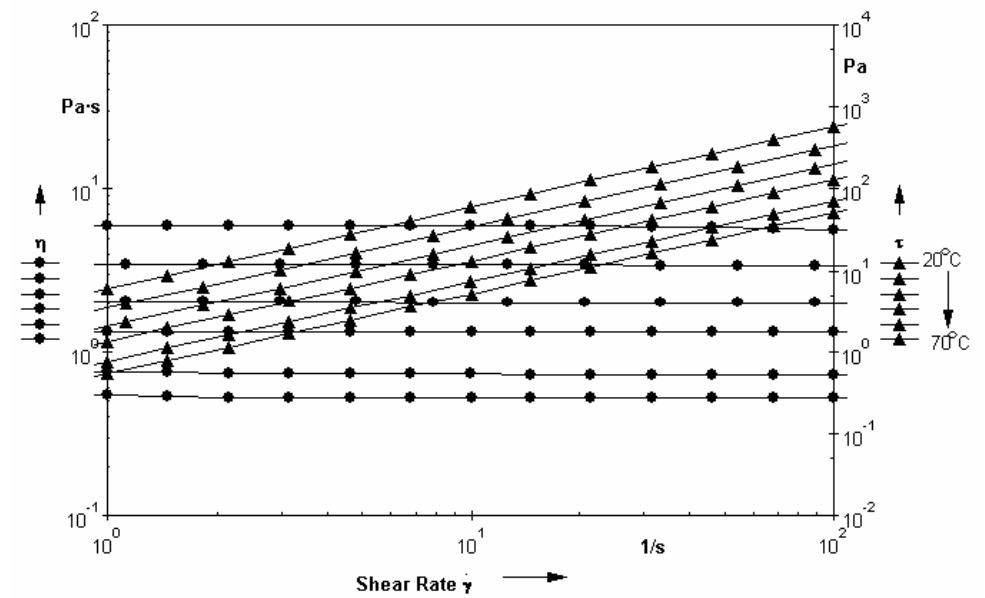


Fig. 7 – Flow/viscosity curves at $t$ = 20, 30, 40, 50, 60, 70°C, in the shear rate $\dot{\gamma} = (0.1 - 1000)\ \mathrm{s}^{-1}$ domain, with $B$ = 0 mT – sample MF / UTR-30, $M_s$ = 1100 G.

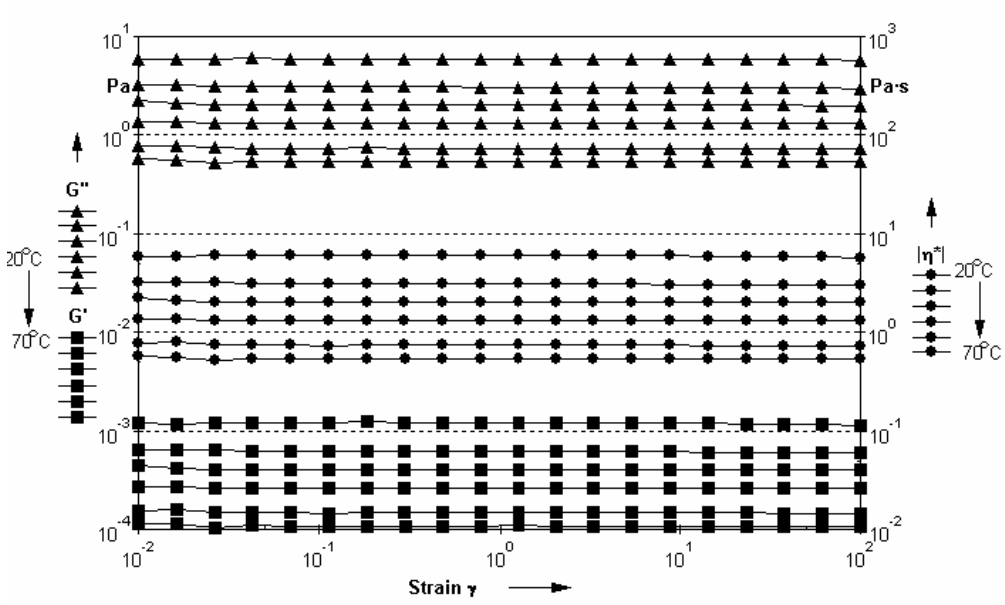


Fig. 8 – Amplitude sweep at $t$ = 20, 30, 40, 50, 60, 70°C and $B$ = 0 mT – sample MF / UTR-30, $M_s$ = 1100 G.

$G'' = G''(\omega)$ curves obtained in the frequency sweep test at the same temperatures, $\gamma_A = 1$ and $B = 0$ mT are shown in Fig. 9.

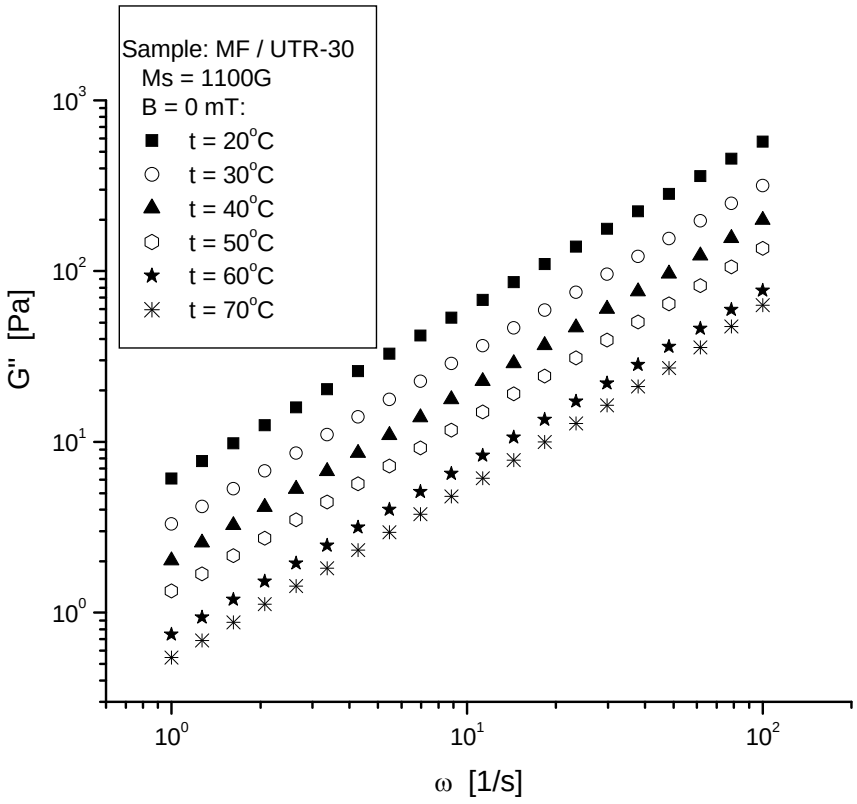


Fig. 9 – Results for frequency sweep tests at $t = 20, 30, 40, 50, 60, 70^{o}$C and $B = 0$ mT – sample MF / UTR-30, $M_s = 1100$ G.

The horizontal shift factor $a_T$ was determined in the same way as for the MF / UTR-30, $M_s = 600$ G sample.

Knowing $a_T$, the vertical shift factor $b_T$ was determined with a linear fit of $\log G''(T_0, \omega) = f(\log \omega)$:

$$\log G''(T_0, \omega) = A + B \cdot \log \omega .$$

The data sets for other temperatures were then shifted, "reduced", over the data for the reference temperature $T_0 = (20 + 273.15)$ K:

$$\log G''(T,a_T,\omega)=A+B\cdot\log(a_T,\omega),$$

where

$$G''(T,a_T,\omega)\ =\ b_T G''(T,\omega)\Rightarrow\ b_T\ =\ \frac{G''(T,a_T,\omega)}{G''(T,\omega)}.$$

Here we already know $a_T$, and $G''(T,a_T,\omega)$ is determined using $G''(T,a_T,\omega)\ =\ 10^{A+B\log(a_T,\omega)}$ (and then considering the average of the values obtained for all angular frequencies).

By shifting the data on the horizontal and vertical axes we obtain the master curve of Fig. 10.

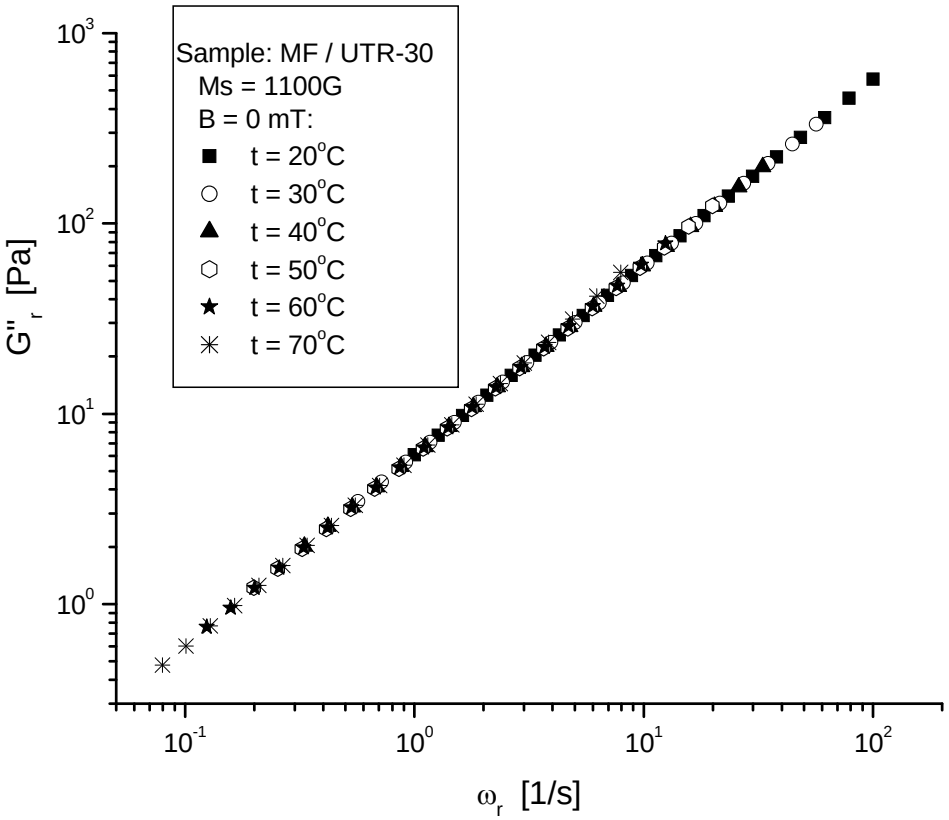


Fig. 10 – Master curve at $B$ = 0 mT – sample MF / UTR-30, $M_s$ = 1100 G.

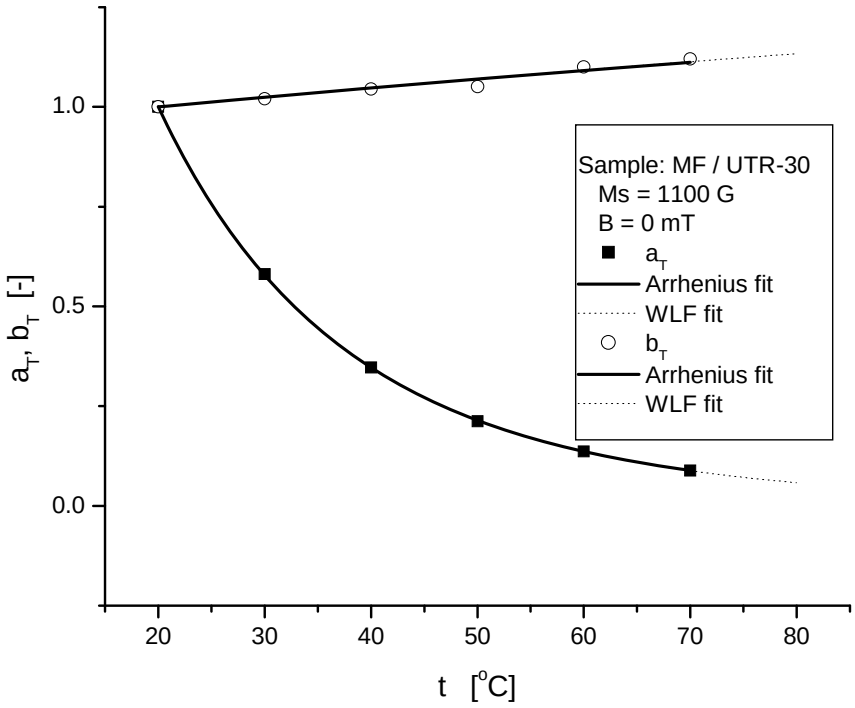


Fig. 11 – The dependence of $a_T$ and $b_T$ factor on temperature at $B$ = 0 mT, sample MF / UTR-30, $M_s$ = 1100 G.

The dependence of the shift factors on temperature is shown in Fig. 11. The data were fitted using the Arrhenius and WLF models, with fitting parameter values from Table 2. We can see that both models fit the data well ($a_T$ was determined from the correlation of viscosity *versus* temperature data with Arrhenius' formula).

*Tabel 2*

Fit equations (and coefficients regression) from Fig. 11

| MF / UTR-30, $M_s$ = 1100 G, $B$ = 0 mT | |
|---|---|
| Arrhenius model | WLF model |
| $\begin{cases} a_T = \exp\left[4863.66\left(\frac{1}{T}-\frac{1}{T_o}\right)\right], R^2 = 1 \\ b_T = \frac{1}{\exp\left[212.98\left(\frac{1}{T}-\frac{1}{T_o}\right)\right]}, R^2 = 0.939 \end{cases}$ | $\begin{cases} a_T = 10^{\frac{-7.84\ (T\ -\ T_o)}{321.13+\ (T\ -\ T_o)}}, R^2 = 0.999 \\ b_T = 10^{\frac{+0.35\ (T\ -\ T_o)}{321.13+\ (T\ -\ T_o)}}, R^2 = 0.940 \end{cases}$ |

*Tests in the presence of a magnetic field*. The same tests were performed for the sample MF / UTR-30 with $M_s$ = 1100 G in an applied field having the magnetic induction values $B$ = 125, 253 and 503 mT. The flow/viscosity curves at $t$ = 20°C given in Fig. 12 indicate a moderate magneto-viscous effect for low fields, but a significant one for the highest value of the magnetic induction, $B$ = 503 mT (especially for low shear rate). At this magnetic field changes also the rheological behavior of the sample, from Newtonian to shear thinning. This evidences the formation of agglomerates which are destroyed progressively for increasing values of the shear rate $\dot{\gamma}$ .

For $I$ = 0.5 A for the electric current in the coil of the magnetorheological cell, which corresponds to $B$ = 125 mT for the induction of the applied magnetic field, following the same steps as in the absence of a magnetic field, applying TTSP led to the results shown in Figs. 13 and 14.

Temperature dependence of the shift factors $a_T$ and $b_T$ (Fig. 15) is similar to the one we had in the absence of the magnetic field. Both models (Arrhenius and WLF) fit $a_T = f(t)$ better than $b_T = f(t)$, as it can be seen from the results presented in Table 3. In this case also the dependence of $a_T$ on temperature is stronger than that of $b_T$.

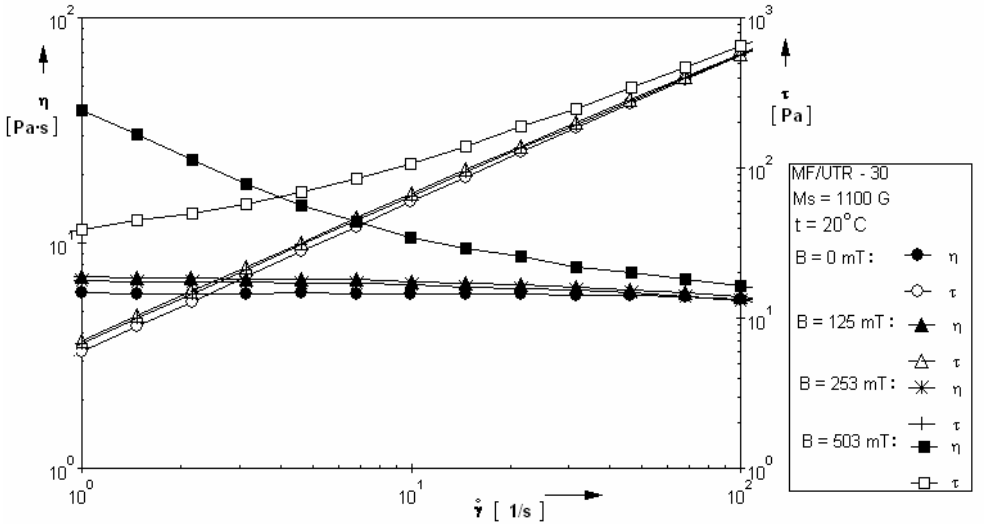


Fig. 12 – Flow / viscosity curves at $t$ = 20°C and $B$ = 0, 125, 253, 503 mT; sample MF / UTR-30, $M_s$ = 1100 G.

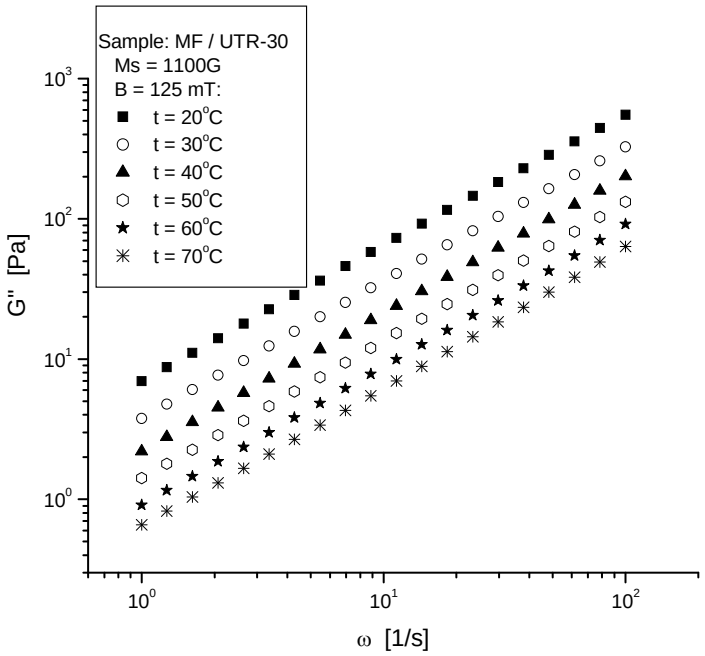


Fig. 13 – Results for frequency sweep tests at various temperatures and $B$ = 125 mT, sample MF / UTR-30, $M_s$ = 1100 G.

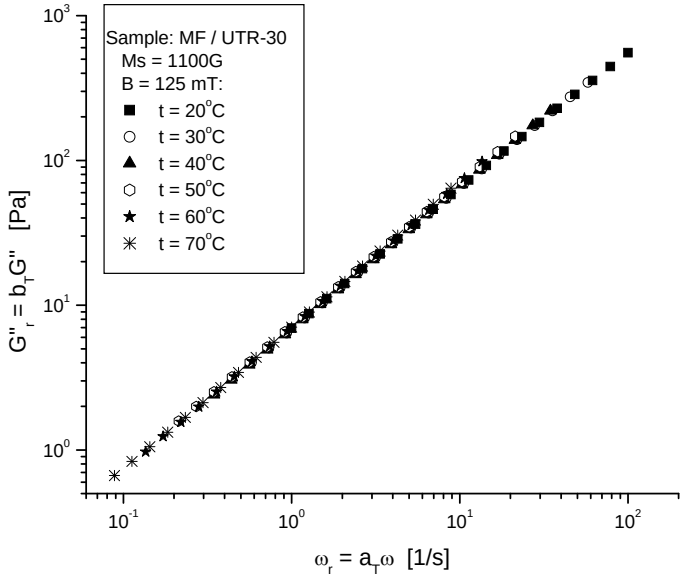


Fig. 14 – Master curve at $B$ = 125 mT – sample MF / UTR-30, $M_s$ = 1100 G.

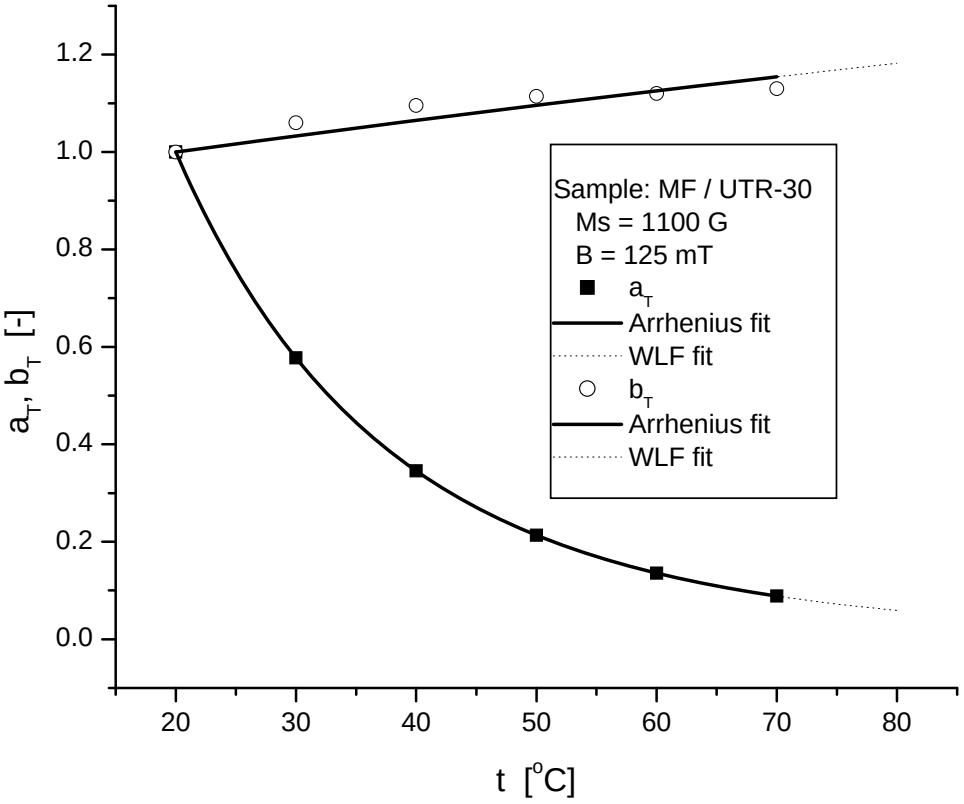


Fig. 15 – The dependence of factors $a_T$, $b_T$ on temperature at $B$ = 125 mT, sample MF / UTR-30, $M_s$ = 1100 G.

*Tabel 3*

Fit equations (and coefficients regression) from Fig. 15

| MF / UTR-30, $M_s$ = 1100 G, $B$ = 125 mT | |
|---|---|
| Arrhenius model | WLF model |
| $\begin{cases} a_T = \exp\left[4876.71\left(\frac{1}{T}-\frac{1}{T_o}\right)\right], R^2 = 1 \\ b_T = \frac{1}{\exp\left[288.84\left(\frac{1}{T}-\frac{1}{T_o}\right)\right]}, R^2 = 0.782 \end{cases}$ | $\begin{cases} a_T = 10^{\frac{-7.23\ (T\ -\ T_o)}{293.19+\ (T\ -\ T_o)}}, R^2 = 1 \\ b_T = 10^{\frac{+0.43\ (T\ -\ T_o)}{293.19+\ (T\ -\ T_o)}}, R^2 = 0.782 \end{cases}$ |

Similar results for the same sample when we apply TTSP were obtained at $I = 1$ A ($B = 253$ mT) – Figs. 16–18 and Tabel 4.

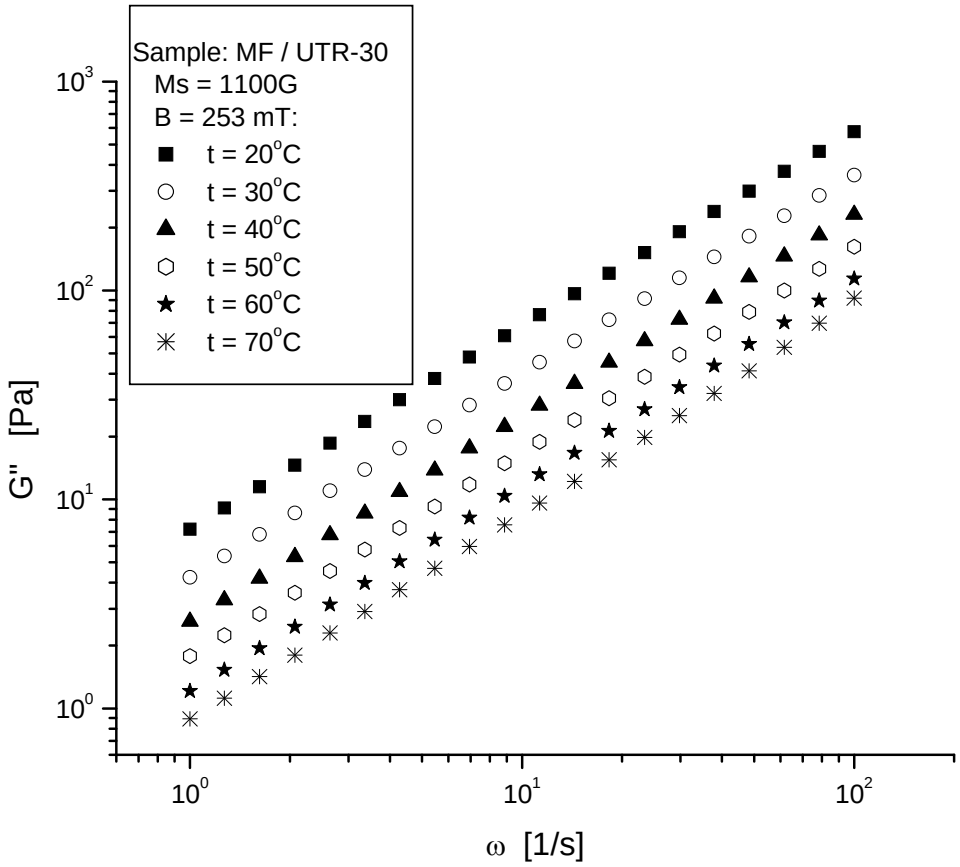


Fig. 16 – Results for frequency sweep tests at various temperatures and $B = 253$ mT, sample MF / UTR-30, $M_s = 1100$ G.

Therefore, even in the presence of a low intensity external magnetic field the validity of TTSP is confirmed, even with a high concentration of magnetite particles in the magnetic nanofluid in which particle agglomerates were revealed [5].

Thus, another advantage of TTSP is the prediction of values for some rheological quantities not only at low angular frequencies, but also at values within the investigated domain for magnetic fields ($B \leq 253$ mT) and for all temperatures considered.

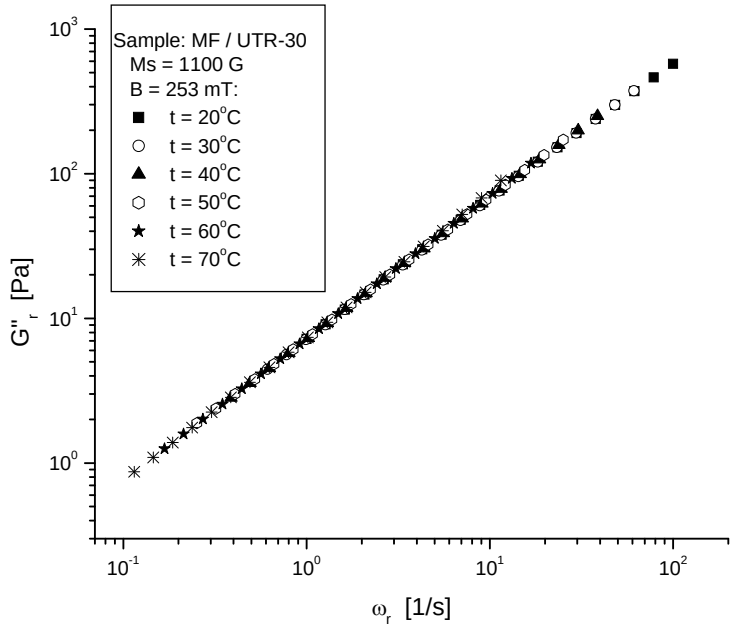


Fig. 17 – Master curve at $B$ = 253 mT – sample MF / UTR-30, $M_s$ = 1100 G.

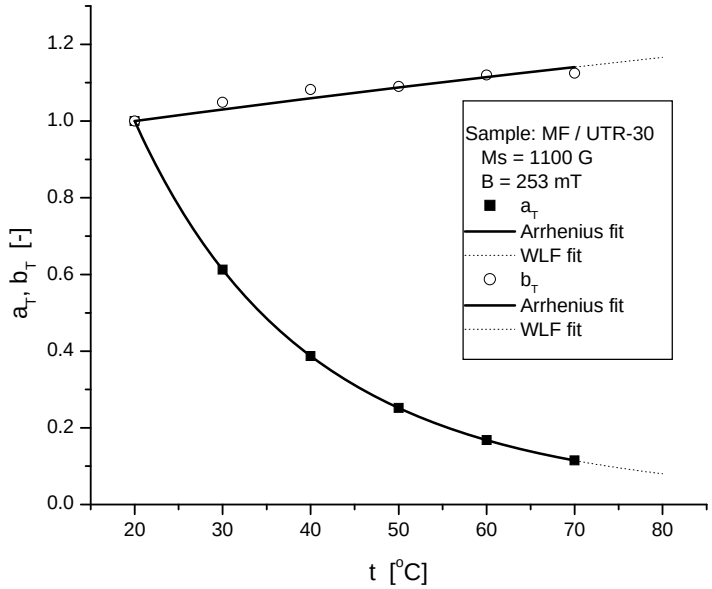


Fig. 18 – The dependence of factors $a_T$, $b_T$ on temperature at $B$ = 253 mT – sample MF / UTR-30, $M_s$ = 1100 G.

*Tabel 4*

Fit equations (and coefficients regression) from Fig. 18

| MF / UTR-30, $M_s$ = 1100 G, $B$ = 253 mT | |
|---|---|
| Arrhenius model | WLF model |
| $\begin{cases} a_T = \exp\left[4354.13\left(\frac{1}{T}-\frac{1}{T_o}\right)\right], R^2 = 1 \\ b_T = \frac{1}{\exp\left[265.19\left(\frac{1}{T}-\frac{1}{T_o}\right)\right]}, R^2 = 0.882 \end{cases}$ | $\begin{cases} a_T = 10^{\frac{-6.45\ (T-T_o)}{293.12+(T-T_o)}}, R^2 = 1 \\ b_T = 10^{\frac{+0.39\ (T-T_o)}{293.12+(T-T_o)}}, R^2 = 0.882 \end{cases}$ |

The dependency of shift factors $a_T$ and $b_T$'s on magnetic field induction $B$ within the investigated temperature domain for this sample is very weak (as opposed to the dependence on temperature), as seen in Fig. 19.

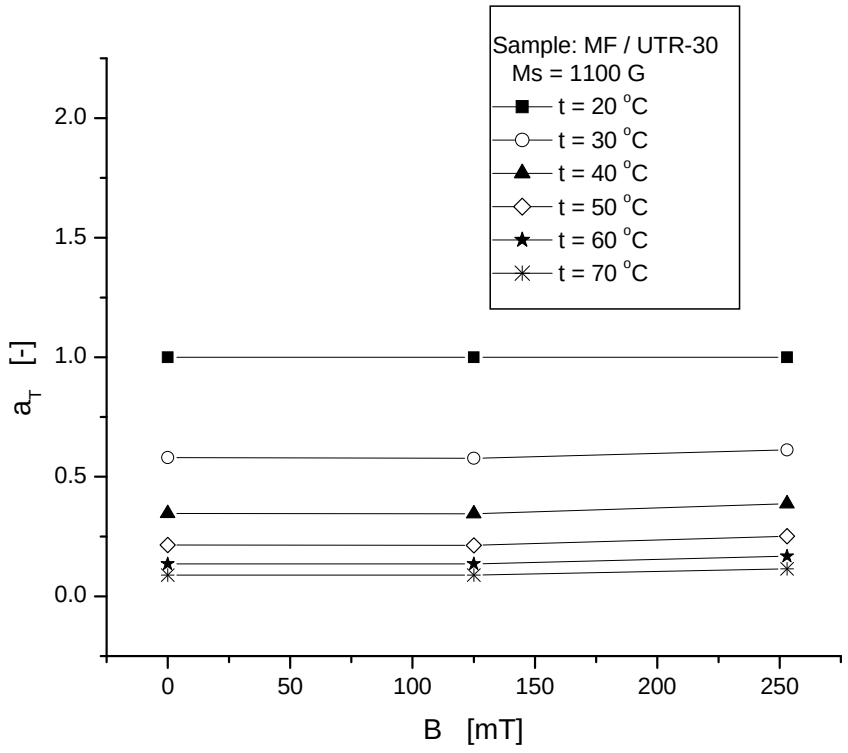


a)

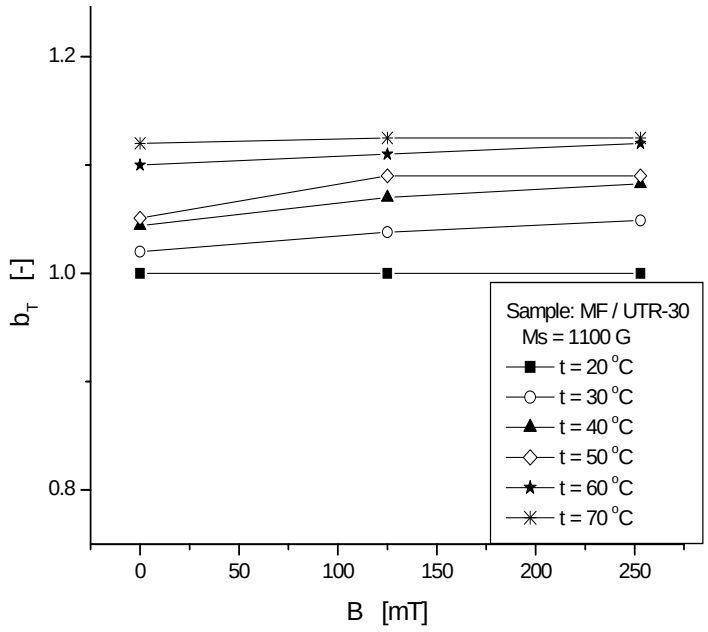


b)

Fig. 19 – Shift factor: a) $a_T$ and b) $b_T$ dependency on applied magnetic field induction $B$, at all temperatures investigated – sample MF / UTR-30, $M_s$ = 1100 G.

We tried to apply TTSP for this sample for higher values of magnetic field induction in the MR cell, $I$ = 2A which corresponds to magnetic induction $B$ = 503 mT. Results for flow/viscosity, amplitude sweep and frequency sweep tests are shown in Figs. 20, 21, 22. We can see from these plots that the rheological behavior of sample MF / UTR-30, $M_s$ = 1100 G changes under the influence of an intense external magnetic field.

- The flow behavior becomes shear thinning, more pronounced at higher temperatures, and the viscosity increases with increasing of magnetic field induction, as illustrated in the flow/viscosity curves of Fig. 20. This indicates the formation of particle agglomerates induced by the intense magnetic field which break when strain increases; break-up is also favored by the increase of the temperature.
- The storage modulus *G'* becomes comparable in magnitude with the loss modulus *G",* especially at low strain, so the sample becomes viscoelastic – Fig. 21.
- The loss modulus *G"* dependency on angular frequency ω also changes in aspect when compared to previous cases – Fig. 22; it is no longer linear, and the data sets obtained from the Frequency sweep tests at different temperatures are no longer parallel. Therefore, they can no longer be shifted over a reference temperature, as it was done previously.

We conclude that the TTS principle cannot be applied for this concentrated MF in the presence of an intense external magnetic field; consequently, the nanofluid is no longer a thermo-rheological simple material in this case.

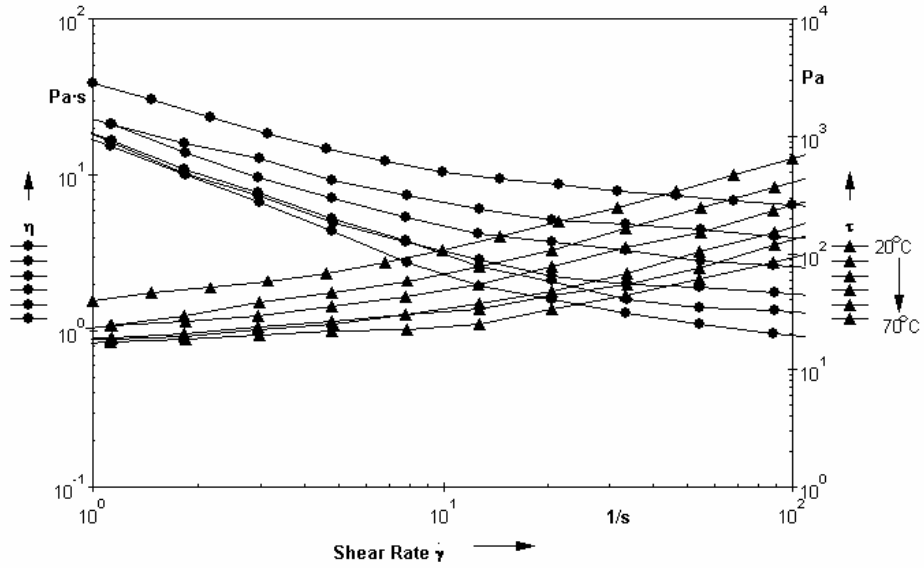


Fig. 20 – Flow/viscosity curves at temperatures $t$ = 20, 30, 40, 50, 60, 70°C, with shear rates in the domain $\dot{\gamma} = (1-1000)$ s$^{-1}$, at $B$ = 503 mT – sample MF / UTR-30, $M_s$ = 1100 G.

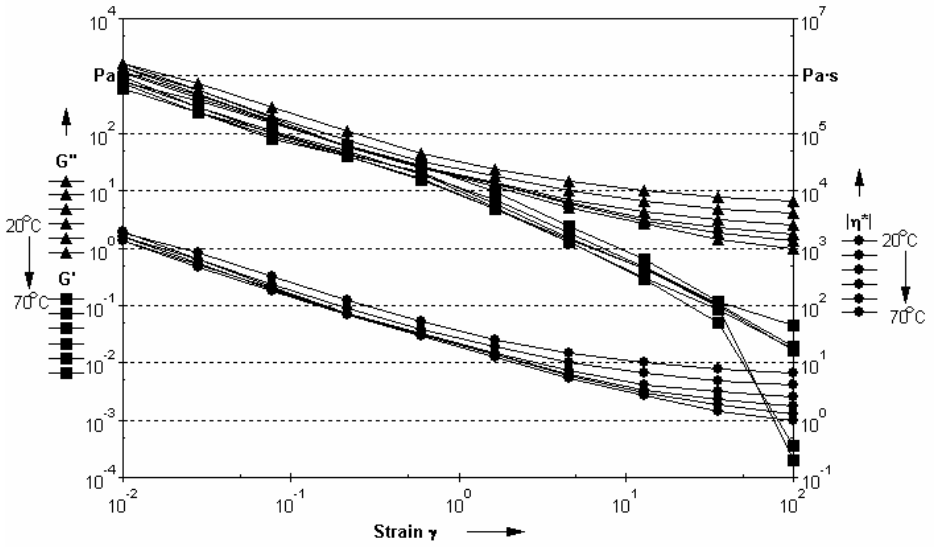


Fig. 21 – Amplitude sweep at the same temperatures and $B$ = 503 mT – sample MF / UTR-30, $M_s$ = 1100 G.

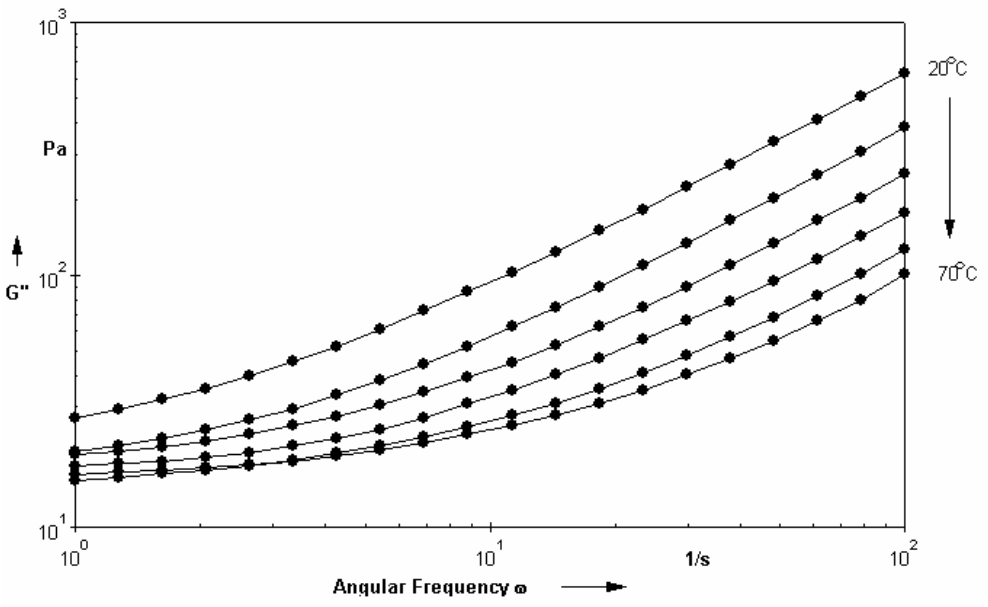


Fig. 22 – Frequency sweep test results at various temperatures and $B$ = 503 Mt, sample MF / UTR-30, $M_s$ = 1100 G.

## 4. CONCLUSIONS

Magnetic fluids with high saturation magnetization and relatively low viscosity are required in many engineering applications and the knowledge of rheological and magnetorheological behavior is important for their use in well controlled conditions.

The prediction of flow properties of magnetic fluids when the temperature and/or the magnetic field induction change is important for most of the magnetic fluid devices, therefore checking the thermo-rheological character of these fluids in the absence and presence of an external magnetic field can offer a sound support in establishing exploitation strategies of magnetic fluids.

Following the investigation of the rheological behavior of two concentrated samples of MF / UTR with $M_s$ = 600 G and $M_s$ = 1100 G respectively, we obtained highly reliable results in the absence of an external magnetic field. For the sample with $M_s$ = 600 G, both shift factors were determined experimentally from the temperature dependency of the viscosity and density of the sample.

For the sample with $M_s$ = 1100 G only $a_T$ could be determined experimentally, and $b_T$ was obtained by shifting the data sets. It was possible to analyze the high concentration sample even in the presence of an applied magnetic field and TTSP was validated up to magnetic induction of $B$ = 253 mT. For values

higher than $B$ = 253 mT, all rheological tests reveal an intensification of particle agglomeration, and the simple thermo-rheological character is lost.

For both samples it is shown that horizontal shift factor $a_T$'s variation with temperature is stronger than that of vertical shift factor $b_T$, as it was reported in previous papers. The temperature dependencies of the two factors follow both an Arrhenius type formula and the WLF formula. For the sample with $M_s$ = 1100 G, the dependence of the shift factors on the magnetic induction B is negligible.

Therefore, the flow properties of the samples (one with very high concentration) are still adequate for their use in rotating seals or other applications that require high concentration nanofluids, even in the presence of a low intensity external magnetic field.

In conclusion, the application of the TTS principle for the rheological characteristics of a MF (respectively, the simple thermo-rheological character), has several advantages. It allows to determine values for rheological quantities at low angular frequencies (where measurements are difficult to perform and take long periods of time), as well as to determine these values for any temperature in the investigated domain. At the same time, TTSP allows to predict the rheological characteristics not only for low angular frequencies, but also for values of applied magnetic fields within the investigated interval ($B \leq$ 253 mT) and for any temperature in the analyzed domain.

***Acknowledgments.*** This work was supported by the Research Program LLM-CCTFA 2013-2015 of the Romanian Academy. The critical comments and helpful suggestions of Dr. Ladislau Vékás are gratefully acknowledged. The author is indebted to Florica Balanean (Potra) for the preparation of MF samples and to Dipl.-Phys. Oana Marinica, PhD fellow for the VSM measurements.

REFERENCES

1. S. Odenbach, *Ferrofluids*, in: K.H.J. Buschow (Ed.), *Handbook of Magnetic Materials*, **16** (Ch. 3), 127–208 (2006).
2. G. Bossis, O. Volkova, S. Lacis, A. Meunier, *Magnetorheology: Fluids, Structures and Rheology*, in: S. Odenbach (Editor), *Ferrofluids: Magnetically controllable fluids and their applications*, Lecture Notes in Physics (Springer-Verlag), **594**, 202–232 (2002).
3. L. Vékás, *Ferrofluids and Magnetorheological Fluids* (review), Advances in Science and Technology, **54**, 127–136 (2008).
4. J. de Vicente, D.J. Klingenberg, R. Hidalgo-Álvarez, *Magnetorheological Fluids: A Review*, Soft Matter, **7**, 3701–3710 (2011).
5. D. Susan-Resiga, V. Socoliuc, T. Boros; T. Borbáth; O. Marinica; A. Han, L. Vékás, *The Influence of Particle Clustering on the Rheological Properties of Highly Concentrated Magnetic Nanofluids*, Journal of Colloid & Interface Science, **373** (*1*), 110–115 (2012); (doi: 10.1016/j.jcis.2011.10.060).
6. D. Susan-Resiga, D. Bica, L. Vékás, *Flow behaviour of extremely bidisperse magnetizable fluids*, J. Magn. Magn. Mater., **322**, 3166–3172 (2010).

7. D. Susan-Resiga, L.Vékás, *Yield stress and flow behavior of concentrated ferrofluid based magnetorheological fluids: the influence of composition*, Rheologica Acta, 2014 (to appear); doi: 10.1007/s00397-014-0785-z.
8. T. Borbáth, D. Bica, I. Potencz, I. Borbáth, T. Boros, L. Vékás, *Leakage-free Rotating Seal Systems with Magnetic Nanofluids and Magnetic Composite Fluids Designed for Various Applications*, Int. J. of Fluid Machinery and Systems, **4**, *1*, 67–75 (2011).
9. J. Delay and D. Plazek, *Time-Temperature Superposition – A Users Guide*, Rheology Bulletin, **78**, *2*, 16–31 (2009).
10. R. Miranda Guedes, *A viscoelastic model for a biomedical ultra-high molecular weight polyethylene using the time-temperature superposition principle*, Polymer Testing, **30**, 294–302 (2011).
11. R. Miranda Guedes, *Analysis of temperature and aging effects on biomedical ultrahigh molecular weight polyethylene's grades using a viscoelastic model*, Polymer Testing, **30**, 641–650 (2011).
12. M. Oroian, S. Amariei, I. Escriche, G. Gutt, *A Viscoelastic Model for Honeys Using the Time–Temperature Superposition Principle (TTSP)*, Food Bioprocess Technol, **6**, 2251–2260 (2013); doi: 10.1007/s11947-012-0893-7.
13. M.L. Williams, R.F. Landel, J.D. Ferry, *The temperature dependence of relaxation mechanisms in amorphous polymers and other glass-forming liquids*, Journal of the American Chemical Society, **77**, *14*, 3701–3707 (1995).
14. A. Vananroye, P. Leen, P. Van Puyvelde, C. Clasen, *TTS in LAOS: validation of time-temperature superposition under large amplitude oscillatory shear*, Rheologica Acta, **50**, *9–10*, 795–807 (2011).
15. P.E. Rouse, *A theory of the linear viscoelastic properties of dilute solutions of coiling polymers*, J. Chem. Phys., **21**, 1272–1280 (1953).
16. F. Bueche, *Viscosity self-diffusion and allied effect in solid polymers*, J. Chem. Phys., **20**, 1959–1964 (1952).
17. P. Wood-Adams and S. Costeux, *Thermorheological behaviour of polyethylene: Effects of microstructure and long chain branching*, Macromol., **34**, 6281–6290 (2001).
18. D. Bica, I. Potencz, L. Vékás, G. Giula, F. Potra, Romanian Patent RO 115533 B1, 2000.
19. L. Vékás, M.V. Avdeev, D. Bica, in: Donglu Shi (Ed.), *NanoScience in Biomedicine*, Springer, USA, 2009, p. 645.
20. R.E. Rosensweig, *Ferrohydrodynamics*, Cambridge Univ. Press, Cambridge, 1985, p. 344.
21. B.M. Berkovsky, V.F. Medvedev, M.S. Krakov, *Magnetic fluids – Engineering applications*, Oxford University Press, 1993, p. 2.
22. D. Bica, *Preparation of magnetic fluids for various applications*, Romanian Reports in Physics, **47**, *3–5*, 265–272 (1995).